Hospital and urban wastewaters shape the structure and active resistome of environmental biofilms

Elena Buelow[1,2], Catherine Dauga[3,4*], Claire Carrion[5], Hugo Mathé-Hubert[1], Sophia Achaibou[4], Margaux Gaschet[2], Thomas Jové[2], Olivier Chesneau[6], Sean P. Kennedy[3], Marie-Cecile Ploy[2], Sandra Da Re[2], Christophe Dagot[2]

1 Univ. Grenoble Alpes, CNRS, UMR 5525, VetAgro Sup, Grenoble INP, TIMC, 38000 Grenoble, France

2 INSERM, CHU Limoges, RESINFIT, UMR1092, University of Limoges, Limoges, France

3 Institut Pasteur, Université Paris Cité, Département Biologie Computationnelle, F-75015 Paris, France

4 Biomics Pole, CITECH, Institut Pasteur, F-75015 Paris, France

5 University of Limoges, INSERM; CHU Limoges, UMR CNRS 7276, F-87000 Limoges, France

6 Collection de l'Institut Pasteur (CIP), Microbiology Department, Institut Pasteur, Paris 75015, France

* present address: Institut Pasteur, University Paris Cité, Department of Virology, Arboviruses and Insect Vectors, F-75015 Paris, France

Abstract

We studied hospital and urban wastewater (WW) biofilms *in situ* and in an *in vitro* laboratory model to assess and compare their potential to actively disseminate and express ARGs. Biofilms were subjected to confocal microscopy to qualify and quantify their extracellular polymeric substances (EPSs), including polysaccharides, external DNA (eDNA), and lipids. We observed that antibiotic challenge had a differential impact on the EPS and the live-dead ratios of *in vitro* hospital and urban WW biofilms. Differential expression of a range of antibiotic resistance genes (ARGs) and mobile genetic elements (MGEs), including those on plasmids, was assessed using a meta-transcriptomic approach. Expression of ARGs as well as MGEs, *in situ,* was 10-fold higher in hospital WW biofilms compared with urban, suggesting a higher frequency of ARG transfer might occur in hospital WW. *In vitro* data confirmed that the addition of ciprofloxacin significantly increased ARG and MGE expression in hospital but not in urban WW biofilms suggesting that the regulation of ARG and MGE expression is likely dependent on the structure and composition of the biofilm. The different responses to antibiotic pressure in hospital *vs* urban biofilms, coupled with differences in biofilm structure helps delineate distinct characteristics of hospital and urban WW biofilms.

Introduction

Biofilms are the preferred lifestyle of bacteria in the natural environment. They present structures that support high densities of bacteria, exhibit high tolerance to antimicrobials, and facilitate gene transfer (1–3). In aquatic environments, biofilms are suggested to serve as hot spots for the accumulation and dissemination of antimicrobial resistance genes (ARG) (1,4). Chemical pollutants spread by urban, industrial, and agricultural waste exert a continuous selective pressure on the diverse antibiotic resistance gene (ARG) pool present in the natural environment and its microbial communities (5–7). For example, ciprofloxacin is a very stable molecule often found in anthropogenically polluted environments and enriched in wastewater (WW), particularly hospital WW (7–10). Ciprofloxacin is not efficiently removed by WW treatment through activated sludge (11); it can be detected in WW and downstream aquatic environments and was identified to pose a significant risk for selection of antimicrobial resistance (AMR) in these environments (9,10,12). Furthermore, ciprofloxacin is known to induce the SOS-response in Gram-negative bacteria. This induction of the SOS response can lead to the expression of antibiotic resistance genes as the quinolone resistance-encoding *qnrB* gene, or the expression of genetic elements as the class 1 integron integrase gene, leading to ARG cassette rearrangements (13,14). In addition, bacteria that are present in the human gut carry a wide variety of ARGs that can be spread into the environment by human feces through WW (15–18). To limit the dissemination of chemical pollutants, pathogens and ARGs into the environment, the implementation of WW treatment systems worldwide plays a key role (6,19–22). However, WW treatment plants are also regarded as selection and dissemination hot spots due to the high density of human gut, environmental bacteria, and chemical pollutants (22–24). Biofilms in WW systems represent an important source of ARGs and bacteria that may end up circulating in the environment and hence present an important model to study the dissemination of resistance in the context of discharged effluents (4,25,26). Biofilms dominate most habitats on earth, accounting for ~ 80% of all bacterial and archaeal cells (27). Biofilm communities are typified by high densities of bacteria embedded in a self-produced protective matrix, which contributes to high antibiotic tolerance, and facilitates gene transfer (4,28). Extracellular polymeric substances (EPS), such as external DNA (eDNA), proteins, lipids, and polysaccharides, are essential structural components of the biofilm matrix that are involved in resilience to antibiotics and exogenous stress, but also in horizontal gene transfer (HGT) (29–31). Previous studies have shown that hospital WW contain significantly higher amounts of resistant bacteria, ARGs and mobile genetic elements (MGEs), as well as chemical and pharmaceutical pollutants compared to urban WW. However, these quantities are generally diluted when hospital WW is mixed with urban WW in community sewer systems (7,32,33).

62 Demonstration of the transfer, dynamics, and regulation of ARGs and MGEs in a complex environmental
63 matrix is yet experimentally challenging, with many essential open questions such as how and when
64 transfer and dissemination of ARGs occur in nature. The extent and conditions of MGE transfer that carry
65 ARGs is still largely unexplored in natural environments and microbial communities. In this study we
66 implemented a sampling and analysis approach that allows phenotypic and genomic analyses of *in situ*
67 and reconstituted *in vitro* hospital and urban wastewater (WW) biofilms. To better understand the role of
68 hospital and urban WW biofilms in actively disseminating antimicrobial resistance in the WW system, we
69 explored the extracellular polymeric substances (EPS) within the biofilm matrix, the biofilm composition
70 (microbiota), the resistome (antibiotic, biocide, and heavy metal resistance genes) and mobilome (mobile
71 genetic elements), with focus on expressed genes (metatranscriptome).

72 ## Materials and Methods

73 **Sample collection and biofilm production *in situ* and *in vitro*:**

74 Wastewater (WW) biofilm production campaigns (*in vitro* and *in situ*) were conducted in January 2017.
75 For *in vitro* biofilms, 20L of untreated urban (up flow of the WWTP Limoges city), and hospital (900-bed,
76 Limoges teaching hospital France) WW were collected on the same day and transported (at 4°C) to the
77 laboratory for immediate use in continuous biofilm reactors. The remaining WW was stored at 4°C to
78 replace evaporated volume every two days. For each WW type, two reactors containing 3L of WW were
79 fed at a continuous rate, from an external container containing the same WW (5L in total), ensuring
80 circulation and a stable level in the biofilm reactors (closed continuous system) (Supplementary Figure 1).
81 Rooms were kept darkened, and the temperature was maintained at 17°C. Sixteen polystyrene slides
82 suitable for confocal laser scanning microscopy (CLSM) (Agar Scientific LTD, UK) were attached to a rotator
83 that was constantly turning, producing 16 biological replicate biofilms per reactor. After 3 days of initial
84 biofilm formation, 1µg/L of ciprofloxacin (considered as the minimum selective concentration (MSC) of
85 ciprofloxacin for most environmental bacteria (34) was added to one reactor for each biofilm type (urban,
86 hospital, lab duplicate). On day 7, the urban and hospital biofilms grown in the reactors containing
87 ciprofloxacin were challenged with a fresh dose of ciprofloxacin (1 µg/L) and harvested the same day (D7)
88 4 hours after ciprofloxacin challenge. Samples were processed within 30 minutes after harvesting. For
89 metagenomics analysis, 8 biological replica biofilms were scraped with tissue cell scrapers (Biologix®) from
90 the slides and washed/suspended in 1X phosphate buffered saline solution (PBS), transferred in 2ml
91 Eppendorf tubes, and immediately shock frozen in liquid nitrogen. Samples were stored at -80°C until
92 RNA/DNA extraction. For CLSM analysis, the remaining 8 slides were washed gently once with 1x PBS and

93 either directly stained (for life/dead staining) or fixed in 3.7% formaldehyde solution for 1 hour and
94 preserved for subsequent EPS staining.

95 For *in situ* biofilms, holes were drilled into polystyrene slides ends and attached with fishing line (16 slides
96 in total, Supplementary Figure 1). The string of polystyrene slides was immersed into the hospital WW
97 pipe and attached at the access point. Slides were recovered after 7 days. Slides were separated and
98 carefully collected in a slide box containing cooled 1xPBS solution and transported to the laboratory
99 immediately for processing. Slides that showed sufficient biofilm formation (by eye) and were least
100 polluted with residues of tissue and other large waste debris, were immediately scraped from the slides
101 and shock frozen in liquid nitrogen as described above. Remaining slides were washed gently in 1xPBS and
102 fixed in 3.7% formaldehyde solution for 1 hour for subsequent EPS staining and CLSM analysis. The same
103 procedure was applied for the *in situ* biofilm production in the untreated urban WW directly at the WWTP
104 (slides were attached and emerged in the large WW receiving pipe/body after primary water filtration
105 step (removal of large debris)). Slides were recovered as described above and stored in a slide box
106 containing cooled 1xPBS. At least four suitable biofilm slides/replicates were directly processed on site by
107 scraping them from the slides and shock freezing them in a portable liquid nitrogen tank. The remaining
108 slides were transported at 4°C to the laboratory and fixed in 3.7% formaldehyde solution for subsequent
109 EPS staining and CLSM analysis as described below.

110 **Sample processing:**

111 DNA extraction was performed with the DNA/RNA dual extraction kit (Qiagen) according to the
112 manufacturer's instructions and stored at -20°C. RNA quality, as measured by RNA integrity number (RIN)
113 was insufficient for RNA sequencing. Therefore, RNA was extracted from remaining biological replicates
114 and samples using the ZymoBIOMICS DNA/RNA Miniprep Kit. DNA concentration was determined by
115 Qubit Fluorometric Quantitation (Thermo fisher scientific, Waltham, MA USA) assays according to the
116 manufacturer's instructions. All DNA samples were diluted or concentrated to a final concentration of 10
117 ng/µl for downstream qPCR and 16S rRNA analysis. RNA concentration and integrity were analyzed by the
118 Agilent 2100 Bioanalyzer system.

119 **High-throughput qPCR for clinical resistome analysis:**

120 Nanolitre-scale quantitative PCRs to quantify genes that confer resistance to antimicrobials were
121 performed as described previously (7,32,35). We targeted 76 genes, grouped into 16 resistance gene
122 classes; targeted genes include ARGs that are prevalent in the gut microbiota of healthy individuals (15),

123 clinically relevant ARGs (extended-spectrum β-lactamases (ESBLs), carbapenemases, and vancomycin
124 resistance), and heavy metals and quaternary ammonium compounds resistance genes suggested to favor
125 cross and co–selection for ARGs in the environment (36,37). We also targeted 11 other targets, including
126 common transposase gene families and class 1, 2 and 3 integron integrase genes, that are important
127 vectors for ARGs in the clinics and often used as proxy for anthropogenic pollution (38). This set of 87
128 genes constituted what we named the targeted resistome (Supplementary Table 1). We also included
129 primers targeting 16S rDNA. Primer design and validation prior to and after Biomark analysis has been
130 done as described earlier (7,35). Real-Time PCR analysis was performed using the 96.96 BioMark™
131 Dynamic Array for Real-Time PCR (Fluidigm Corporation, San Francisco, CA, U.S.A) as described previously
132 (7). Thermal cycling and real-time imaging were performed at the Plateforme Génomique GeT – INRA
133 Transfert (https://get.genotoul.fr/en/), and Ct values were calculated using the BioMark Real-Time PCR
134 analysis software. Calculations for normalized and cumulative abundance of individual genes and
135 allocated gene classes were performed as previously described (7,32,35). The resistome data displayed
136 here and used for statistical analysis is based on resistome data that was obtained for two biological
137 replicates per sample.

138 **16S rRNA gene sequencing and sequence data pre-processing**

139 Extracted DNA samples for 16S rRNA sequencing were prepared following a dual barcoded two-step PCR
140 procedure for amplicon sequencing for Illumina. The V4 region was sequenced by generating 2 x 300 bp
141 on an Illumina MiSeq. Data was demultiplexed and filtered for quality and remaining primers according to
142 recommended practices as described previously (7).

143 **16S rRNA data analysis**

144 Illumina MiSeq forward and reverse reads were processed using the MASQUE pipeline
145 (https://github.com/aghozlane/masque). Briefly, raw reads are filtered and combined followed by
146 dereplication (dereplication is the identification of unique sequences so that only one copy of each
147 sequence is reported) Chimera removal and clustering are followed by taxonomic annotation of the
148 resulting OTUs by comparison to the SILVA database. A BIOM file is generated that combines both OTU
149 taxonomic assignment and the number of matching reads for each sample. Relative abundance levels for
150 bacterial taxa (family/genus level) were obtained and analyzed (7).

151

152 **Metatranscriptomics and RNA sequencing:**

153 Cell pellets were re-suspended in TRIzol reagent and subjected to three cycles of 1min bead-beating
154 (0.5mm silica/zirconia beads) followed by RNA extraction using the Direct-zol RNA Kit (Zymo research)
155 according to the manufactures' protocol. DNA was removed by TURBO DNase (Ambion) until no genomic
156 DNA was detected by PCR. The quality and integrity of the total RNA were checked on the Bioanalyzer
157 system (Agilent). Because RNA yield is low, only 6 samples containing the highest amount of RNA and best
158 RIM values (>6) were selected for RNA sequencing and meta-transcriptomic analysis (data not shown).
159 Ribosomal RNA depletion was performed using the Bacteria RiboZero kit (Illumina). From rRNA-depleted
160 RNA, directional libraries were prepared using the TruSeq Stranded mRNA Sample preparation kit
161 following the manufacturer's instructions (Illumina). Libraries were quantified on Bioanalyzer DNA chips
162 (Agilent) and Qubit® dsDNA HS Assay Kit (ThermoFisher). 150 bp paired read sequences were generated
163 on the Nextseq 500 (high output) sequencer according to manufacturer's instructions (Illumina). The
164 multiplexing level was 10 samples per lane. Reads were cleaned for low-quality and adapter sequences
165 using Cutadapt version 1.11.

166 The level of ribosomal RNAs (rRNAs) remained high in our environmental samples, even after both *in vitro*
167 rRNA depletion step and optimized RNA extraction methods (see above). We tackled these technical
168 shortcomings by including an *in-silico* rRNA depletion step to improve mRNA read assembly and
169 subsequent analysis (Supplementary Fig. 2 and Supplementary Tables 2 and 3). Ribosomal RNA reads
170 were filtered out by mapping on the Silva database with BWA-MEM v0.1.17 (default parameters) and
171 Samtools v1.9 (36). Then, unmapped reads (mRNA) were subjected to *de novo* assembly using SPADES
172 v3.13.1 (k-mer length 21). From 31% to 42% of trimmed reads coding for rRNA per sample were fast
173 assigned to bacterial families with Kraken (39) against the Silva SSU/LSU-Ref database (Release 132) (40).
174 27% to 31% of reads corresponded to not classifiable metagenomics sequences, related to microbial dark
175 matter (41). 0.68% to 12% of reads were classifiable on the 16S rRNA Silva database. (Supplementary
176 Figure 6, Supplementary Table 3).

177 After sequencing, trimming and *in silico* ribosomal RNA depletion, we obtained 4.137.706 putative mRNA
178 reads (57.77 % of the initial sample) for the Hospital *in situ* biofilm, and 35.861.826 putative mRNA reads
179 (29.6% of the initial sample) for the Urban *in situ* biofilm, leading to a reasonable number of contigs to
180 analyse, with 866.221 and 2.379.394 contigs for the hospital and urban WW *in situ* biofilms, respectively
181 (Supplementary Table 2). For the hospital WW *in vitro* biofilms HL-1 and HL-2 (HL-2 = hospital WW *in vitro*
182 biofilm with ciprofloxacin added) 14.860.486 and 36.452.020 mRNA reads were obtained leading to

183 2.332.472 (HL-1) and 3.285.208 (HL-2) assembled contigs, respectively. For the urban WW *in vitro* biofilms
184 UL-1 and UL-2 (UL-2= urban WW *in vitro* biofilm + ciprofloxacin), 55.513.773 and 38.054.494 mRNA reads
185 were obtained leading to 3.483.745 and 2.684.771 assembled contigs, respectively (Supplementary Table
186 2 and 3).

187 **Metatranscriptomic analysis:**

188 Mapping the mRNA assemblies to specific reference databases enables to assess the expression levels of
189 functionally viable ARGs within biofilms.

190 A specialized database of the genes targeted by the high-throughput qPCR for the targeted resistome
191 analysis was built (accession numbers available in Supplementary Table 1) and used for mapping
192 assembled contigs with BWA-MEM v0.1.17 (with default parameters) and SAMtools v1.9. Then, the
193 transcriptome activity and abundance of ARGs was assessed by mapping reads on assembled contigs (42).
194 Reads were mapped against each ARG-like sequence identified from meta-transcriptomic assembly
195 contigs, using Bowtie2 v2.3.4.3 with default settings. The ARG-like sequences with > 100 mapped reads
196 were assigned to ARG transcripts.

197 To increase the chance of detecting active ARGs in hospital and urban wastewater biofilms, transcripts
198 coding for ARGs were searched against the CARD database (release 08/21/2019) by using the Resistance
199 Gene Identifier (RGI 3.1.0) retaining perfect and strict hits only (43). The ARG-like sequences were
200 identified as ARG transcripts when their coverage was up to 80% with a minimum of 100 reads mapping.
201 The expression level of a particular ARG transcript in each sample was calculated by summing the number
202 of hits by ARG class (see list of categories in Supplementary table 3). In addition, we weighted the
203 identification with the mean of read coverage by ARG class.

204 In addition, we detected ARG-carrying MGEs in WW biofilms, namely the active resistance mobilome.
205 First, assembled contigs were mapped against the ACLAME database (44), using BWA and Samtools.
206 Subsequently, identified MGE-carrying contigs were again mapped against the CARD database to identify
207 ARG-carrying MGEs. If one MGE-carrying contig mapped to different ARGs, only hits with the best CIGAR
208 (extracted from the SAM file) were considered.

209 All steps described above were implanted in python-based modules, and all modules formed the
210 framework of the pipeline AROM, for ARg On Mobilome (Supplementary Figure 2). Lately, we added the
211 module get abundance to normalize gene expression levels according to the sample size (Gb), the length
212 of reads and the length of each ARG (45). All changes to AROM

213 (https://github.com/sophiaachaibou/ARGmodules) are tracked in GitHub and the versions managed using
214 bioconda.

215 **Extracellular polymeric substances (EPS) staining for confocal scanning laser microscopy:**

216 The following stains were used to fluorescently label EPS components (polysaccharides, lipids, and
217 external DNA) and to assess live-dead ratios of different biofilm samples. Life-dead: Propidium Iodide (red;
218 0.5µM working solution) and SYTO-BC (green; Life technologies™; 5uM working solution). 500µl of each
219 fluorescent dye applied and allowed to incubate at ambient temperature in the dark for 30 min. Slides
220 were subsequently rinsed with three times with PBS and immediately analyzed by CSLM. For the EPS
221 components, biofilms were fixed in 3.7% formaldehyde solution (see above) prior to EPS staining. For
222 external DNA (eDNA) the combination of TOTO-1 (green) and SYTO-60 (red) (Life technologies™) was used.
223 Staining was performed as described by Okshevsky et *al.* (46), by using a final working stock solution (in
224 phosphate buffered saline (PBS)) of TOTO-1 at 2µM and SYTO-60 at 10µM. Here, following three PBS
225 washes, slides kept at 4°C in the dark until CSLM analysis the same day. For polysaccharides (carbohydrate
226 binding proteins) and proteins a combination of Concanavalin A, tetramethylrhodamine conjugate (ConA;
227 Thermo Fischer Scientific) selectively binding to α-mannopyranosyl and α-glucopyranosyl residues
228 (carbohydrates) and Fluorescein isothiocyanate isomer I (FITC; Siegma Aldrich) selectively binding to
229 proteins was used. FITC working solution was concentrated at 200µg/ml. 500µl of 0.1M sodium
230 bicarbonate buffer was added to the biofilm slide prior to adding 500µl of FITC staining solution (2µg/ml)
231 and incubated at RT in the dark for 30 minutes. Afterwards the excess stain was removed by washing the
232 biofilm slide gently with 1 x PBS solution for three times. Subsequently 500µl of ConA staining solution
233 (50µg/ml) was added to the slide and incubated for 30 minutes at RT in the dark. Excess stain was removed
234 by washing three times with 1x PBS solution. Slides were stored at 4°C until CSLM analysis. For lipid and
235 internal lipid droplet staining Nile Red (0.1µg/ml) was used in combination with FITC (2µg/ml). Incubation
236 and staining were performed as described above by first applying 500µl of 0.1M sodium bicarbonate
237 buffer, subsequently 500µl of FITC working solution, incubation for 30 minutes at RT in the dark, washing
238 with PBS for removal of excess FITC staining and addition of 500µl of Nile Red working solution, incubation
239 for 30 minutes at RT in the dark, removal of excess dye by washing with PBS 3 times, and storing at 4°C
240 until analysis by CSLM.

241

242 **Confocal scanning laser microscopy settings and analysis:**

243 Z stacking acquisitions were acquired with a confocal microscope (ZEISS LSM880) using a x20 and x100
244 magnification. Five Z stacks were performed per condition. The following settings were used to measure
245 the fluorescence from the samples: autofluorescence (λexc 405nm/λem 460nm), FITC (λexc 488nm/λem
246 525nm), tetramethylrhodamine (λexc 561nm/λem 580nm), Nile Red (λexc 641nm/λem 650nm), Syto60
247 (λexc 641nm/λem 678nm) and TOTO-1 (λexc 514nm/λem 533nm).

248 3D view analysis was performed with the Imaris software (Oxford Instrument) using acquisitions with the
249 x20 magnification. Surfaces were created using a manual thresholding. The quantitative analysis was
250 performed with the open-source software BiofilmQ (https://drescherlab.org/data/biofilmQ/) on the
251 acquisitions made with the x100 magnification. Each fluorescent z-stack was segmented using an
252 automatic thresholding (otsu algorithm) allowing object detection and measurements. We focused on the
253 relative abundance parameter that is the measurement of the proportion (i.e a percentage) of one
254 component (i.e one staining) regarding the biovolume. This biovolume must be understood as the total
255 volume occupied by one or the other staining of interest (this is a boolean operation "OR" between these
256 stainings). The relative abundance of the polysaccharides (corresponding to the concanavalin A staining)
257 and the lipids (i.e nile red staining) were expressed as a percentage of the biovolume resulting from the
258 merge between concanavalin A OR fluorescein, or between nile red OR fluorescein respectively. eDNA
259 relative abundance was expressed as a percentage of the TOTO-1 staining (i.e eDNA) regarding the
260 biovolume resulting from the merge between TOTO-1 OR SYTO-60 stainings.

261 **Statistical analysis**

262 **Biofilm matrices**

263 To test for the effect of sample origin (hospital vs urban WW), environment (*in situ* vs *in vitro*) and addition
264 of ciprofloxacin on the composition of the biofilm matrices, the relative abundance of three features were
265 measured, the eDNA, lipid and polysaccharides. For each of these features two models were built. The
266 first set of models focused on data obtained without ciprofloxacin and explained the three measured
267 features with the variables 'sample origin' and 'environment', as well as their interactions. The second set
268 of models focused on data obtained in the in vitro environment and explained the three measured
269 features with the variables 'sample origin' and 'ciprofloxacin', as well as their interactions. The last set of
270 models is devised to perform a pairwise comparison of each sample, hence, a different model was built
271 for each pair of samples, with one explanatory variable and two levels, corresponding to the sample ID.

All these tests were based of the Randomization of Residuals in a Permutation Procedure implemented by the R package RRPP.

Pairwise comparison of the normalized abundance of the resistome data using the Tukey HSD test

To compare the relative abundances of genes classes between samples, for each class and biological replicate, we summed the normalized abundances of individual genes per class. Then for each gene class, we fitted the relative abundance with a log linear model with one explanatory variable, and one level for each sample. Finally, we applied pairwise comparisons of samples using the Tukey HSD test implemented by the multcomp R package and p-values were adjusted using the single step method (47).

Correlation of the normalized abundance for ARGs detected by qPCR and their likelihood to be detected by our meta-transcriptomic pipeline

To detect the threshold for normalized abundance values of genes measured by qPCR, below which meta-transcriptomic has a low chance of detecting the gene, we fitted a binomial generalized linear model (GLM) to the mapped reads obtained for individual genes detected by our meta-transcriptomic pipeline, and as explanatory variable, the normalized abundance of the respective genes measured by qPCR. This allowed to obtain a cut-off value for normalized abundance determined by qPCR that is predicted to have a chance of being detected by our meta-transcriptomic pipeline. We also fitted a Poisson GLMM to the exact read maps for genes detected by our meta-transcriptomic pipeline, with the same explanatory variable as in the binomial GLM, and in addition, an observation level random effect, to account for overdispersion (48).

Pairwise comparison of biofilm communities, mobilome and resistome

For the six types of multivariate description of the biofilms, communities (family and genus levels), mobilome (plasmid and gene levels) and resistome (targeted and non-targeted), we compared each pair of samples by measuring the proportion of the Simpson's diversity that was between samples. Simpson's diversity measures the probability that two entities taken at random from the dataset are of the same type. It is calculated as $1 - \sum {f_i}^2$, where values of $f_.$ are the frequencies of the entities. To compute the proportion of this Simpson's diversity that is between a given pair samples A and B, we computed the total diversity using the average of the frequencies of the two samples and the average diversity within the two sample:

$$D_{AB} = 1 - \frac{(1 - \sum {f_{iA}}^2) + (1 - \sum {f_{iB}}^2)/2}{1 - \sum \left((f_{iA} + f_{iB})/2 \right)^2}$$

301 This divergence index turns out to also be the formula of the between population fixation index (F_{ST}) used
302 in population genetics, using alleles frequencies (49). To assess the significance of these divergences, we
303 permuted the read counts 10^5 times while keeping fixed the headcounts for each entity and sample. For
304 each of these permutations, we recomputed the frequencies and the divergence index, to obtain its null
305 distribution under the assumption that the distributions are identical in the two samples.

306 Based on these pairwise dissimilarities, we built UPGMA trees (unweighted pair group method with
307 arithmetic mean). The stability of the trees was assessed by bootstrapping the individual genes.

308 To test the significance of the divergence between samples we used the pair of samples with the lowest
309 divergence as a conservative reference. That is, we computed for each pair of samples, the proportion of
310 bootstrap with the lowest D_AB divergence. Finally, we assessed and tested the correlation between the
311 dissimilarity matrices used to build the UPGMA trees using some Mantel tests (R package ade4).

312 **Correspondence and in between correspondence analysis for ARG detected on plasmids (mobilome)**

313 To analyze the association between the class of the ARGs of the mobilome and the WW origin of the
314 biofilm and their treatment (*in situ*, *in vitro*, with or without ciprofloxacin), we first performed a
315 correspondence analysis (CA; function 'dudi.coa' of the ade4 R package) analyzing the link between the
316 relative abundance of each ARG associated to a MGE. The significance of this association was tested
317 through a χ^2-test with a p-value based on 10^5 Monte Carlo simulations, and its effect size through the
318 Cramér's V statistic, a measure of the association between two categorical variables that varies from 0
319 (no association) to 1 (complete association). Then ARGs were grouped into gene classes, and the
320 association between gene classes and biofilm was investigated by applying between class analysis
321 (function 'bca' of the ade4 R package) to the CA. We refer to this overall analysis as to a between
322 correspondence analysis (bCA) which significance was assessed though a 10^5 permutation test. This bCA
323 recovered 33% of the total association found in the CA.

324

325 **Results**

326 **Effects of minimal selective concentrations (MSC) of ciprofloxacin, sample origin and**
327 **environment, on hospital and urban WW biofilms' extracellular polymeric substances (EPS)**

328 We first analyzed the global structure of the hospital and urban WW biofilms. The EPS (eDNA, lipids and
329 polysaccharides) were visualized by confocal scanning laser microscopy (CSLM). 3-D imaging (IMARIS) and
330 quantitative analysis (Biofilm Q) showed that the EPS significantly differ between their growth
331 environment, namely whether biofilms were grown *in situ* or, as reconstituted biofilms, *in vitro*. We
332 detected different relative abundance of eDNA (in both hospital and urban biofilms compared to their *in*
333 *vitro* counterparts), polysaccharides (for urban *in situ* vs *in vitro* + cip biofilms) and lipids (for hospital *in*
334 *situ* vs *in vitro* biofilms) (Figure 1 and 2, Supplementary Figure 4a and 4b, Supplementary Table 5). We also
335 detected significant differences in the relative abundance of EPS components dependent on the sample
336 origin, meaning between hospital and urban *in situ* WW biofilms, for eDNA, polysaccharides and lipids
337 (Figures 1 and 2, Supplementary Figure 4a and 4b). The relative abundance of eDNA was higher for the
338 hospital *in vitro* biofilms compared to the urban *in vitro* WW biofilms. We also assessed the impact of
339 adding ciprofloxacin on the life-dead ratio and EPS components of the *in vitro* reconstituted hospital and
340 urban WW biofilms. A significant increase of dead cells was detected for the hospital *in vitro* biofilm after
341 adding ciprofloxacin, compared to its control (Supplementary Figure 3). The relative abundance of eDNA
342 was significantly lower in the hospital *in vitro* biofilm exposed to ciprofloxacin and significantly lower for
343 polysaccharides in the urban *in vitro* biofilm exposed to ciprofloxacin compared to their control.

344 These results were random permutation-based pair-wise comparisons of the average relative abundance
345 data extracted for 5 z-stack acquisitions performed per biofilm sample. Finally, we implemented statistical
346 models based on random permutations testing for an effect of co-founding variables, such as the
347 environment (*in situ* vs *in vitro*), sample origin (hospital vs urban) and/or the effect of ciprofloxacin, on
348 the EPS components of these biofilms (Supplementary Table 5). We confirmed that i) the sample origin
349 (type of hospital vs urban WW) has a significant impact on the abundance of polysaccharides and lipids,
350 ii) whether biofilms are grown *in situ* or *in vitro* has a significant impact on the relative abundance of eDNA

351 and iii) ciprofloxacin has a significant impact on the abundance of polysaccharides for both, hospital, and
352 urban *in vitro* biofilms (Supplementary Table 5).

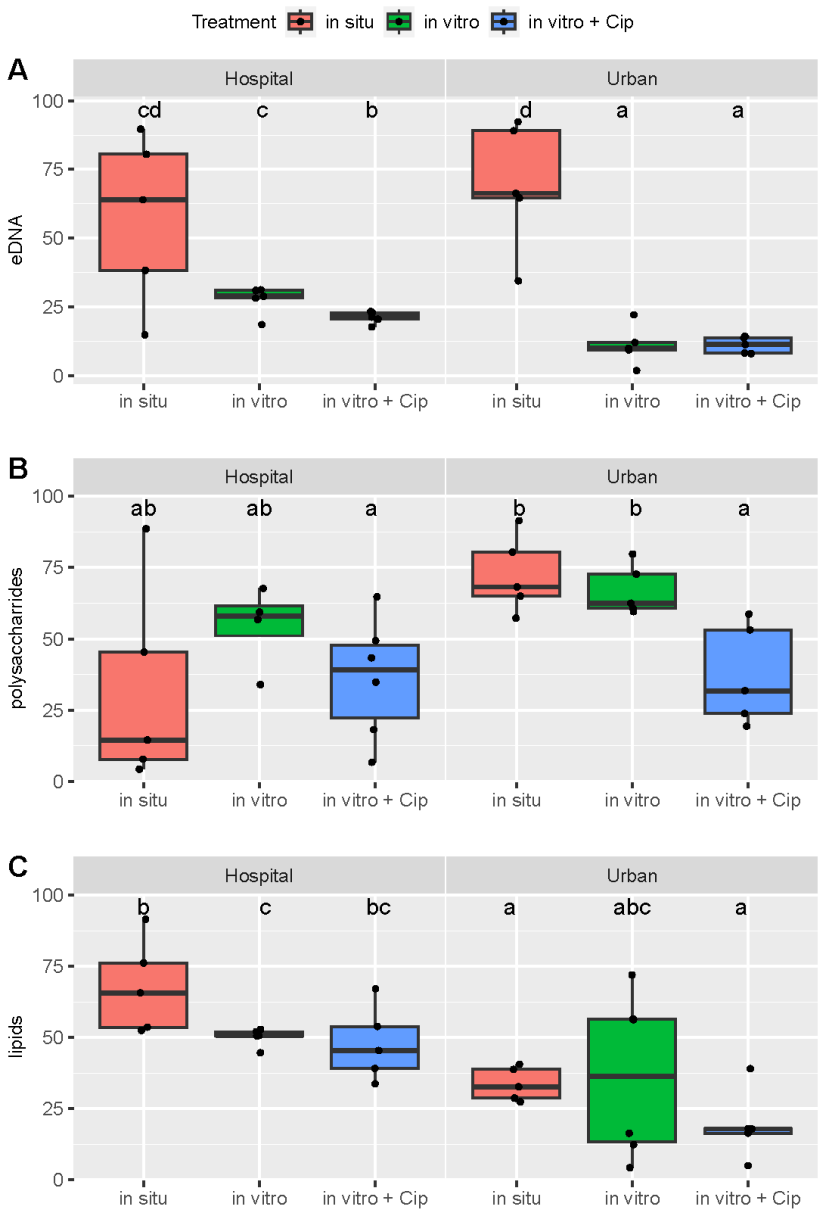

370

371 **Figure 1: Relative abundance of eDNA (A), polysaccharides (B) and lipids (C) in the respective biofilms.** Each EPS
372 component was stained in a different biological replicate, and fluorescence was detected by 5 z-stack acquisitions
373 per biological replicate with a 100-fold magnification for the respective biofilms. Quantitative image analysis was
374 performed with Biofilm Q. Results of pairwise permutations tests are summarized using the compact letter display.
375 Samples that do not share a letter in common are significantly different from each other. +Cip= *in vitro* biofilms were
376 exposed after 3 days of initial biofilm formation with 1 µg/ml ciprofloxacin for 4 consecutive days and harvested
377 after exposure of 4 hours on the final day.

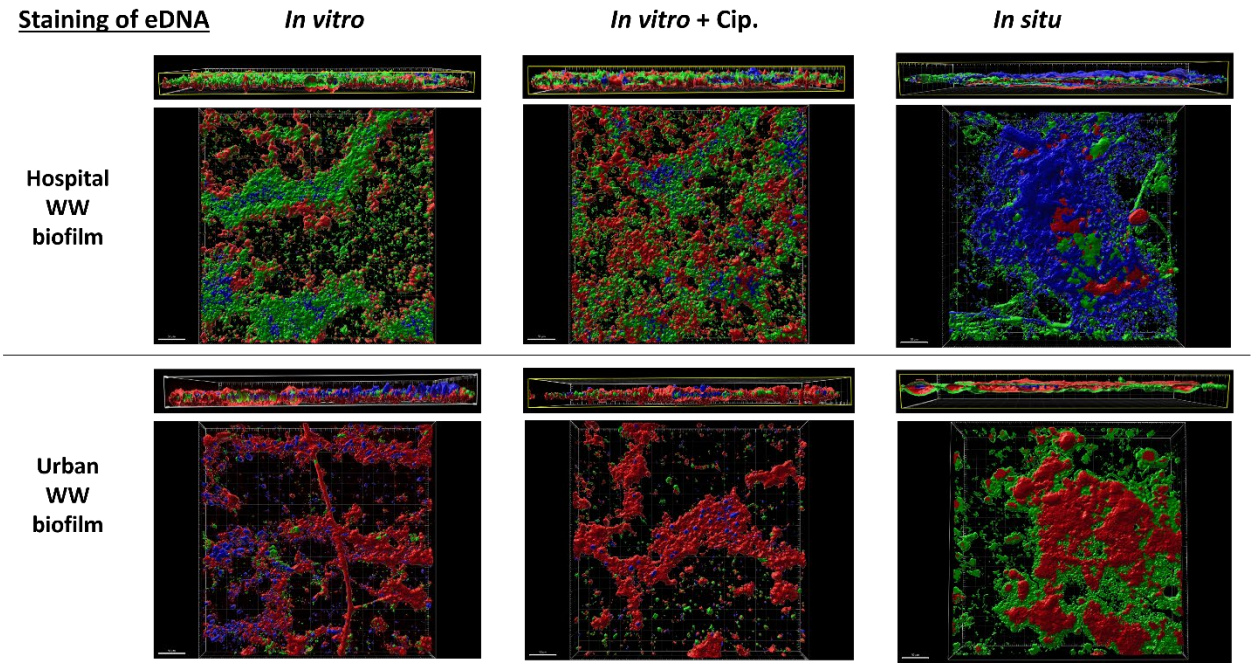

Figure 2: **3D imaging of eDNA (green) and total nucleic acids (red), for hospital and urban *in-situ* and *in-vitro* biofilms.** Autofluorescence for unknown compounds is in blue. +Cip= *in vitro* biofilms were exposed after 3 days of initial biofilm formation with 1 µg/ml ciprofloxacin for 4 consecutive days and harvested after exposure of 4 hours on the final day.

384 **The microbiota of hospital and urban WW *in situ* and *in vitro* biofilms**

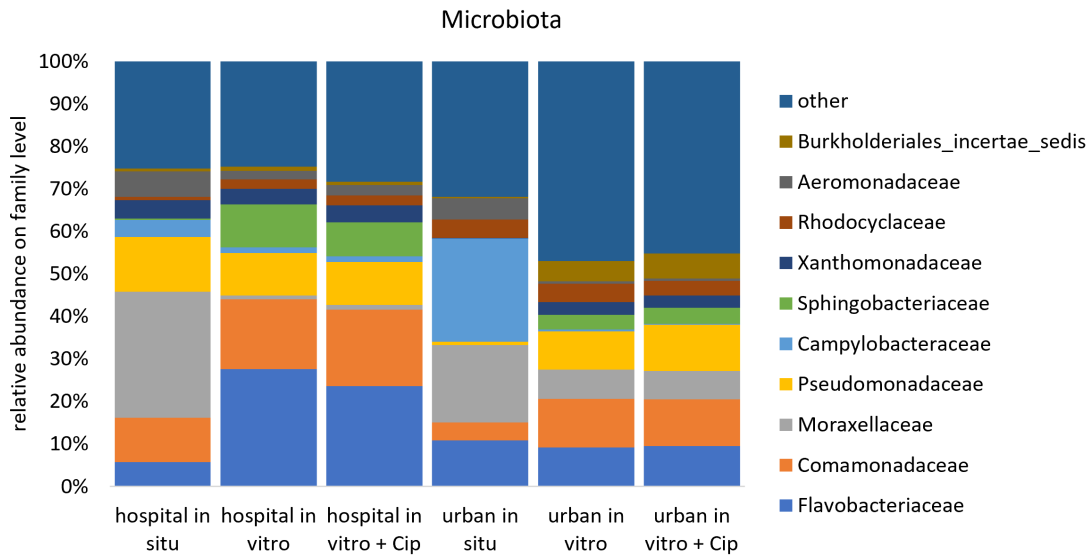

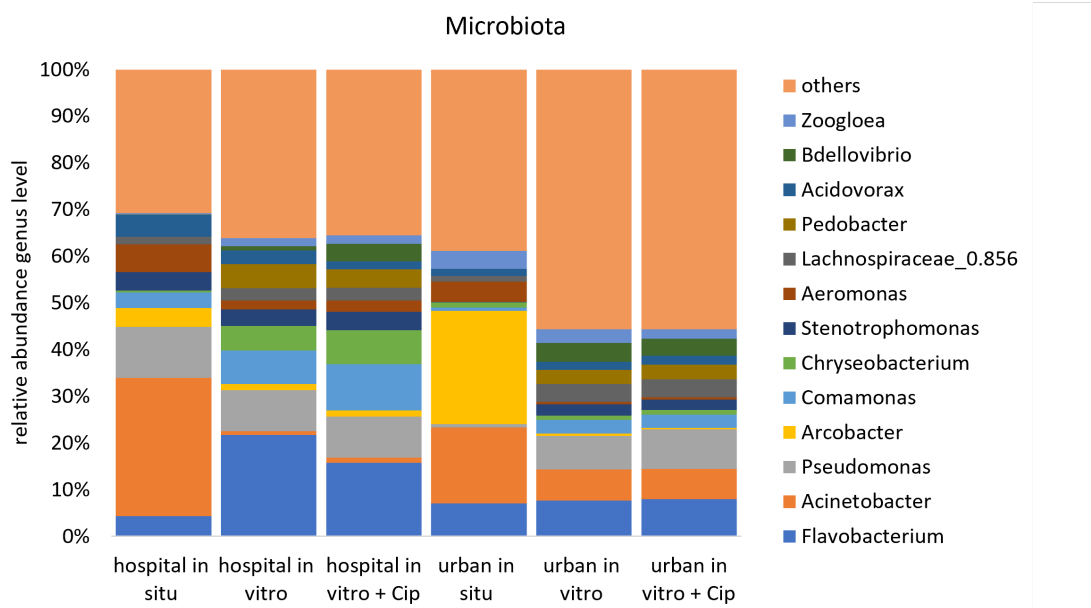

385

386 **Figure 3**: **Microbiota composition of hospital and urban wastewater *in situ* and *in vitro* biofilms based on**
387 **sequencing of the 16S rRNA gene.** Depicted are the top 10 taxa on order level and the top 12 on the genus level for
388 each sample, the remaining taxa are grouped into others. +Cip= *in vitro* biofilms were exposed after 3 days of initial
389 biofilm formation with 1µg/ml ciprofloxacin for 4 consecutive days and harvested after exposure of 4 hours on the
390 final day (D7).

391 The microbial compositions of WW biofilms were assessed using 16S rDNA sequencing. Strikingly and in
392 line with the phenotypic analysis of the biofilm structures, bacterial community profiles of hospital and
393 urban *in situ* biofilms were significantly different from their *in vitro* reconstituted counterparts
394 (Supplementary Figure 5 and Supplementary Table 6). The main genera in the *in situ* hospital WW biofilms

395 are Gram-negative pathogens such as *Pseudomonas*, *Acinetobacter* and *Aeromonas,* responsible for
396 infections in hospitalized patients (50–52) (Figure 3). *In situ* urban WW biofilms are dominated by different
397 genera than hospital WW biofilms, namely *Flavobacterium* and *Arcobacter* but share *Acinetobacter* with
398 hospital *in situ* biofilms. The genus *Arcobacter* is a common member of human WW systems and can rarely
399 act as animal and human pathogen (53,54). It is more abundant in urban WW biofilms, compared to the
400 hospital WW environment. *Pseudomonas* is a dominant genus in both urban and hospital *in vitro* biofilms.
401 Surprisingly, *Acinetobacter* decreased in the *in vitro* biofilms compared to their *in situ* counterparts. The
402 addition of ciprofloxacin did not change the proportional microbiota composition for *in vitro* biofilms
403 compared to their controls (Figure 3), suggesting that exposure of already formed WW biofilms with
404 ciprofloxacin in our *in vitro* model does not alter deeply the primary bacterial ecosystems. However, when
405 assessing Simpson's diversity index and performing pairwise comparison and mantel tests on our 16S
406 rDNA sequencing-based data on the family and genus level, there is evidence that a small proportion of
407 the total microbiota is impacted in its proportional community structure due to the addition of
408 ciprofloxacin in hospital *in vitro* biofilms (Supplementary Figure 5 and Supplementary Table 6).

409 As described in methods, a relatively large proportion of the RNA reads from the metatranscriptomic RNA
410 sequencing approach of the biofilm communities were ribosomal RNA (rRNA) reads. The 16S rRNA reads
411 were filtered out by mapping on the Silva database, allowing for the assignment of a small proportion of
412 those reads (between 0.68% and 12%) on family level. Hence, this step allowed for additional analysis of
413 the "active microbiota" of these biofilms. Among the classifiable 16S rRNA reads from the
414 metatranscriptomic analysis (methods), we identified a large majority of *Enterobacteriaceae* in hospital
415 biofilms and a mix of *Flavobacteriaceae*, *Enterobacteriaceae*, *Streptococcaceae* and *Francisellaceae* in
416 urban *in situ* biofilm (Supplementary Figure 6 and Supplementary Table 3).

417

418

419

The targeted resistome and metatranscriptome in hospital and urban WW biofilms

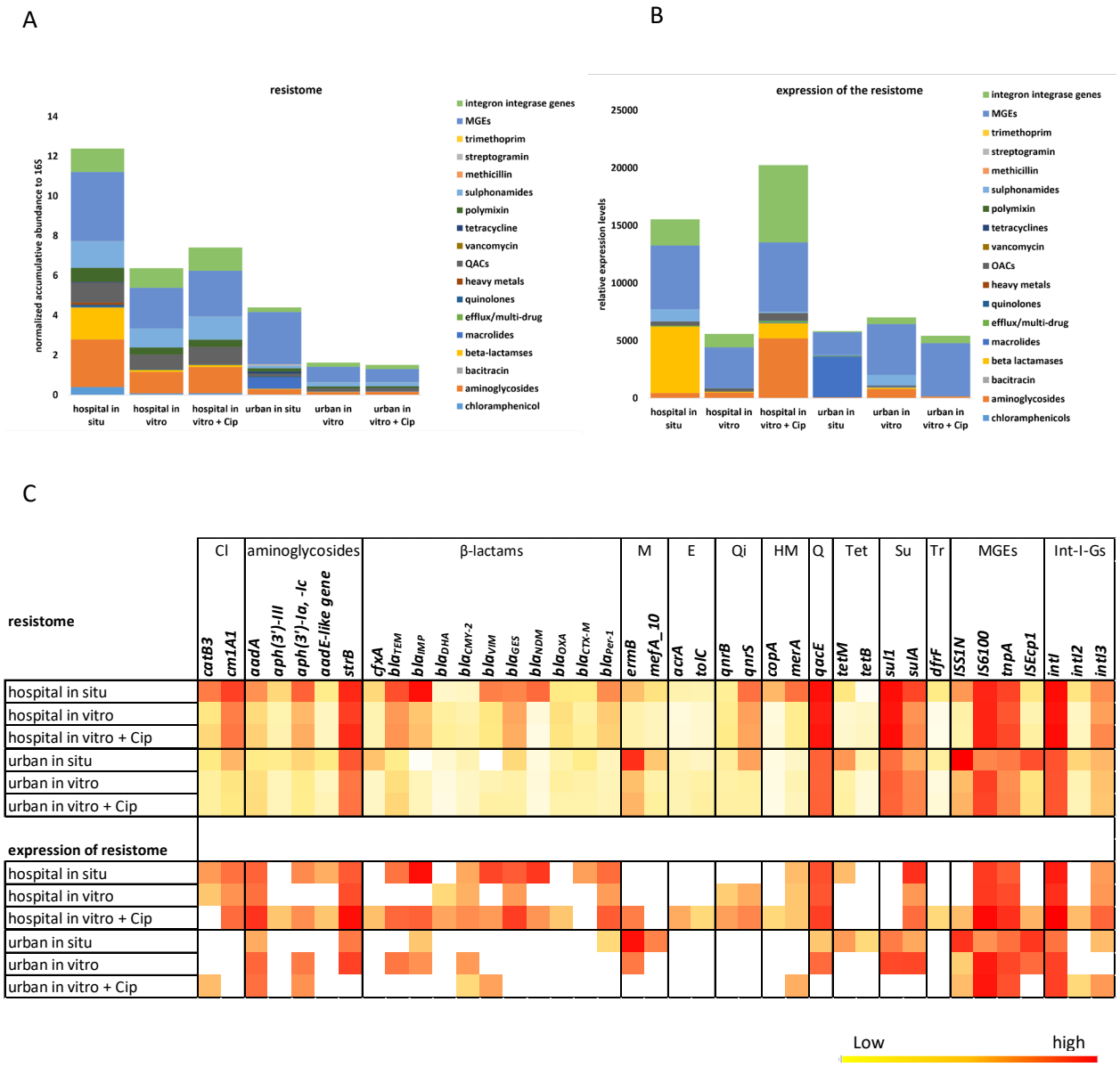

Figure 4: The targeted resistome and its expression in hospital and urban WW biofilms. On panel **A** and **B**, normalized accumulated abundance of the targeted resistome (A) and their relative expression (B) were grouped into gene families and mobile genetic elements (MGEs) and integron integrase genes. **C**: Heatmap depicting normalized abundance of individual genes (targeted resistome) and their normalized expression levels (exact counts of mapped reads for the respective genes) for the individual genes detected by RNA sequencing (meta-transcriptome). Data were log2 transformed for visualization purpose**.** +Ab= *in vitro* biofilms were exposed after 3 days of initial biofilm formation with 1µg/ml of the antibiotic ciprofloxacin for 4 consecutive days and harvested after exposure of 4 hours on the final day (D7). Cl= chloramphenicol; M= macrolides; E= efflux pumps/multi-drug resistance genes; Qi= quinolones; HM= heavy metals; Q= quaternary ammonium compounds (QACs); Tet= tetracyclines; MGEs= Mobile Genetic Elements. Int-I-Gs= integron integrase genes class I, II and III. +Cip= *in vitro* biofilms were exposed after 3 days of initial biofilm formation with 1 µg/ml ciprofloxacin for 4 consecutive days and harvested after exposure of 4 hours on the final day.

437 To assess the resistome in our samples, a targeted high-throughput qPCR approach, that detects and
438 quantifies 87 individual genes conferring resistance to clinically relevant antibiotics, quaternary
439 ammonium compounds (QACs), heavy metals, transposase genes (MGEs) and integron integrase genes,
440 also referred to as targeted resistome, was applied. At first, comparing the different environments in
441 which biofilms grew (*in situ* vs *in vitro*), we found that for the hospital WW biofilms, all gene classes had
442 a higher normalized abundance in *in situ* biofilm compared to the *in vitro* biofilms, except for
443 aminoglycosides, quinolones, QACs, sulphonamides, MGEs and integrons, which were not significantly
444 different (Figure 4 a and c, Supplementary Figure 7, and Supplementary Table 7). Performing the same
445 comparison for the urban WW *in situ* vs the *in* vitro biofilms, the normalized abundances of macrolides,
446 quinolones and MGEs, were significantly higher for the *in situ* biofilms, whereas genes conferring
447 resistance to heavy metals, vancomycin, and sulphonamides had significantly lower normalized
448 abundances in *in situ* urban WW biofilms. Then, comparing the different sampling origin (hospital vs urban
449 WW), the normalized abundance of the targeted resistome was highest in the *in situ* hospital WW biofilms
450 for all detected gene classes apart from macrolides, which were higher in the urban *in situ* biofilm, while
451 tetracyclines, quinolones and MGEs, were not significantly different in their normalized abundance
452 between the two *in situ* biofilm sampling origins (Supplementary Figure 7, and Supplementary Table 7).
453 Comparing the normalized abundance of detected gene classes for the hospital *in vitro* biofilms vs the
454 urban *in vitro* biofilms, it was higher in the hospital *in vitro* biofilms for most genes, except for vancomycin
455 and genes encoding for multi-drug efflux pumps for which the normalized abundance was higher in the
456 urban *in vitro* biofilms; no difference was observed for tetracyclines and heavy metal resistance genes.

457 Then, we analysed the metagenomic messenger RNA (mRNA) to provide information about the targeted
458 resistome actively being expressed in the *in situ* and *in vitro* hospital and urban WW biofilms. Overall, 39
459 of the 87 targeted genes by qPCR were expressed in at least one of the samples (Figure 4b and c).
460 Following the same comparison pattern, when first comparing the biofilm environments (*in situ* vs *in*
461 *vitro*), beta-lactam, chloramphenicol and sulphonamide resistance genes were 112, 5, and 47-fold higher
462 expressed in the hospital *in situ* biofilm vs *in vitro* biofilm, whereas macrolide resistance genes were 49-
463 fold higher expressed in the urban *in situ* biofilm compared to *in vitro* biofilm, while for all other gene
464 classes were gene expression could be detected, these detection levels were lower in the urban *in situ*
465 biofilm vs *in vitro* (Figure 4b and c, Supplementary Table 8 and Supplementary 8). For the different sample
466 origins (hospital vs urban WW) of the studied biofilms, expression levels were higher for 7 gene classes,
467 from 5.5-fold higher for genes conferring resistance to aminoglycosides to 957-fold higher for genes

468 conferring resistance to beta-lactams, (Supplementary Table 8 and Supplementary 8) for the *in situ*
469 hospital vs urban *in situ* WW biofilms.

470 We studied the impact of ciprofloxacin in the *in vitro* biofilm models. When looking at normalized
471 abundance in hospital and urban *in vitro* biofilms exposed to ciprofloxacin, no differences could be
472 detected, except for genes conferring resistance to macrolides in the hospital *in vitro* biofilm exposed to
473 ciprofloxacin compared to its control. (Supplementary Figure 7, and Supplementary Table 7). Interestingly,
474 we observed an enhanced expression of the targeted resistome (Figure 4b and c, Supplementary Table 8
475 and Supplementary Figure 8) after ciprofloxacin addition in the hospital biofilm. For example, expression
476 of ARGs conferring resistance to beta-lactams was 26-fold higher and aminoglycoside resistance genes
477 were expressed 11-fold higher and represented the class of ARGs that was most abundantly expressed
478 proportionally within the hospital biofilm (Figure 4b and c, Supplementary Table 8 and Supplementary
479 Figure 8). Furthermore, ciprofloxacin enhanced expression (4-fold) of the quinolone-resistance genes,
480 *qnrB* and *qnrS* genes, and integron integrase genes (*IntI1* and *IntI3*) by 6-fold and the grouped transposase
481 genes by 1.7-fold compared to its control (Figure 4b and c, Supplementary Table 8 and Supplementary
482 Figure 8). When looking at the detected expression levels of ARG classes in the urban *in vitro* biofilm
483 exposed to ciprofloxacin, expression of ARGs was lower for all detected gene classes apart from the
484 integron integrase and aminoglycoside genes, were expression slightly increased by 1.1 and 1.7-fold
485 respectively, compared to its control (Figure 4b and c, Supplementary Table 8 and Supplementary Figure
486 8). The *ISS1N* gene was specifically expressed in the *in situ* urban WW biofilm.

487 Overall, these findings showed that 45% of the targeted resistome is actively expressed in the WW biofilms
488 and that the expression of ARGs and integron integrase genes in the *in vitro* hospital WW biofilm is
489 enhanced by the addition of ciprofloxacin. Interestingly, the expression level of ARGs could be correlated
490 (linear regression analysis to be R=0.77, Supplementary Figure 10 and Supplementary Table 10) to the
491 normalized abundance of genes determined by the targeted resistome approach until a numerical
492 threshold of 0.057 for the normalized abundance of the individual genes (Supplementary Figure 10 and
493 Supplementary Table 10). Below this threshold, the detection of ARG expression could no longer be
494 achieved, suggesting a lack of transcripts. However, technical limitations such as the low sensitivity of
495 meta-transcriptomics and/or the detection of DNA from dead cells and eDNA by qPCR might also be
496 possible explanations as to why not all the targeted genes could be detected by the metatranscriptomic
497 approach (55–57).
498

499 **Assessing the expression of ARGs based on the CARD database in hospital and urban WW biofilms**

500 To identify additional ARGs that were not included in our targeted resistome approach, mRNA reads of
501 our samples were mapped against the Comprehensive Antibiotic Resistance Database (CARD) that
502 archives thousands of gene sequences encoding resistance determinants to antimicrobial agents.

503 ARG expression was higher for *in situ* hospital WW biofilms compared to their *in vitro* counterpart (10.4%
504 for hospital *in situ* biofilm vs about 0.5% for *in vitro* of total mRNA reads in the respective samples
505 (Supplementary Table 1)). The detected expression levels of ARGs in the *in situ* urban WW biofilms was
506 lower compared to their *in vitro* counterpart (0.04% of mRNA reads for the urban *in situ* vs urban *in vitro*
507 0.4% biofilm). A tenfold higher expression level of ARGs was detected in the *in situ* hospital WW biofilm
508 (10.4 % of all mRNA reads coding for ARGs) compared to the urban WW *in situ* biofilm (0.04 % of mRNA
509 reads coding for ARGs) (Supplementary Table1). For the *in vitro* hospital biofilm exposed to ciprofloxacin,
510 expression level of ARGs was about 4.4-fold higher compared to the non- exposed one (2.4% vs 0.55% vs,
511 (Supplementary Table 1)). No difference in ARG expression level based on total ARG mRNA reads could
512 be observed between urban *in vitro* biofilms exposed or not to ciprofloxacin for the normalized data
513 (0.41% vs 0.37% of total mRNA reads mapping to ARGs, respectively, Supplementary Table 1).

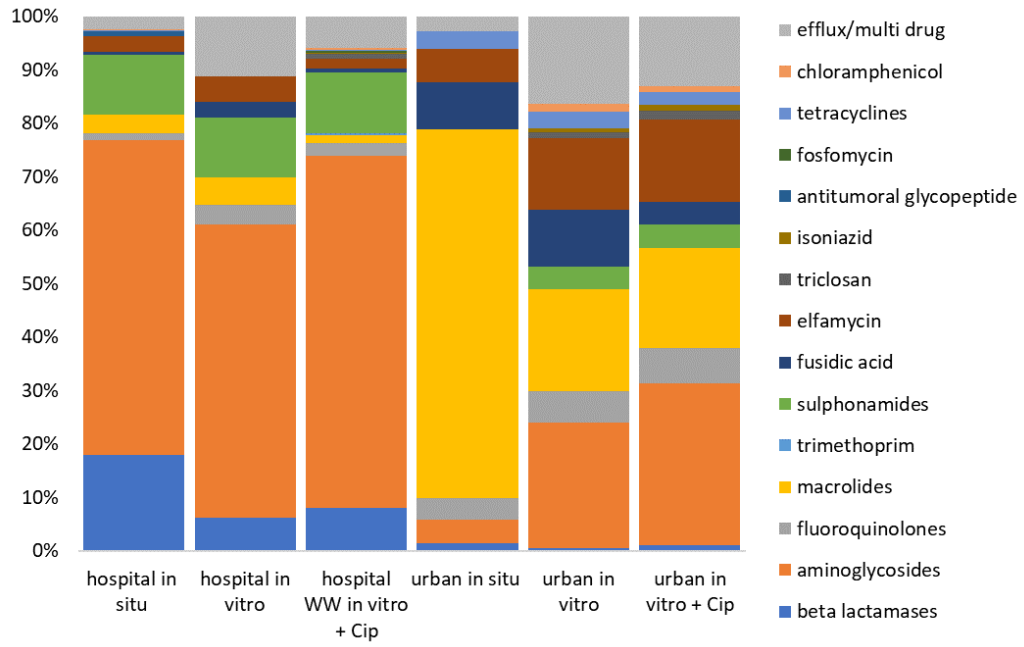

514

515 **Figure 5: ARG metatranscriptome based on the CARD database.** Means of mapped reads per
516 antimicrobial resistance gene were summed by ARG class and are displayed per sample.

517

518 In total we detected the expression of 70 individual resistance genes conferring resistance to 16 classes
519 of antibacterial drugs across all biofilm samples (Figure 5, Supplementary Tables 4 and 9). This approach
520 led to the detection of the expression of additional genes in hospital and urban WW biofilms that were
521 not detected by the targeted approach (Supplementary Table 4). For example, active beta-lactamase such
522 as *bla*^{RCP}, *bla*^{LCR}, *bla*^{FOX}, *bla*^{NPS}, four aminoglycoside-modifying enzymes (*aac(3)-Ib/aac(6')-Ib*, *aad*B,
523 *aph*(3''), *aph*(6)) and a macrolide phosphotransferase (MPH) were identified. Genes that confer resistance
524 to the antimicrobial classes fusidic acid, elfamycin, rifamycin and antitumoral glycopeptides were found
525 to be actively expressed in all the investigated samples. Genes that confer resistance to isoniazid and
526 triclosan were found to be expressed in the *in vitro* hospital biofilm exposed to ciprofloxacin, and in *in*
527 *vitro* urban WW biofilms in both conditions. The expression of an enterobacterial fosfomycin resistance
528 gene (*ptsI*) was detected in the *in vitro* hospital WW biofilm exposed to ciprofloxacin (Supplementary
529 Table 4). Furthermore, the expression of multidrug efflux pumps, specifically RND and MFS types, and the
530 expression of the *bla*^{OXA} beta-lactamases was detected in all the samples.

531 Overall the composition of the ARG metatranscriptome of the CARD resistome analysis correlated to the
532 targeted resistome analysis (Supplementary Figure 5, Supplementary Table 4 and 9). Comparing the
533 different environments for hospital biofilms (*in situ* vs *in vitro*), higher gene expression levels were
534 detected for the *in situ* hospital biofilm between 3.2-fold and 15.2-fold (macrolides and beta-lactamases
535 respectively). For the *in situ* vs *in vitro* urban biofilms, expression levels were lower for all detected ARG
536 classes, apart from macrolide ARGs, which were expressed at a higher level in urban *in situ* biofilm
537 (Supplementary Figure 9, Supplementary Table 4 and 9). For hospital *in situ* biofilm, six ARG classes had
538 between 1.8 and 81.2-fold higher expression levels (genes encoding resistance to fluoroquinolones and
539 aminoglycosides respectively) vs urban *in situ* biofilm. Comparing hospital *in vitro* biofilm exposed to
540 ciprofloxacin to its control, overall, increasing fold-change for seven ARG classes, between 3- and 7.5-fold
541 change for genes encoding for multi-drug efflux pumps and genes conferring resistance to beta-lactams,
542 respectively, was detected. Interestingly, 5 ARG classes, namely aminoglycosides, beta lactams,
543 quinolones, sulphonamides, and genes encoding for multi-drug efflux pumps, were detected to have
544 higher gene expression levels in both, the targeted and non-targeted resistome approach, for the hospital
545 *in vitro* biofilm exposed to ciprofloxacin compared to its control (Supplementary Figures 8 and 9,
546 Supplementary Table 4, 8 and 9). For the urban *in vitro* biofilm exposed to ciprofloxacin, expression levels
547 are lower, expect for genes encoding for beta-lactams were a slight increase (1.18-fold) could be detected
548 compared to its control (Supplementary Figure 9, Supplementary Table 4 and 9).

549 **The active resistance mobilome**

550 To study the expression of MGEs and more specifically MGEs associated with ARGs, assembled contigs
551 were mapped against the plasmid sequence collection v0.4 available at the ACLAME database (44).
552 Subsequently, plasmid associated contigs identified by this approach were mapped back to the CARD
553 database to identify specifically plasmids that carry ARGs. These ARG associated plasmids are referred to
554 as the "active resistance mobilome" in the respective samples.

555 Global expression of plasmids was very low in all the samples studied (0.48% of all assembled contigs for
556 hospital *in situ* biofilm and 0.14% for urban *in situ* biofilm (Supplementary Table 1)). In total, we counted
557 respectively 115 and 66 plasmid-ARG associated contigs for the hospital and urban *in situ* biofilms and
558 identified a diverse range of expressed plasmids (71 individual plasmids identified across all samples)
559 expressing a diverse range of ARGs that could be grouped into 10 classes conferring resistance to
560 antimicrobials, quaternary ammonium compounds and heavy metals. The highest expression level for the
561 active resistance mobilome was observed in the *in vitro* hospital biofilm exposed to ciprofloxacin
562 (Supplementary Figure 11).

563 55 different plasmids carrying a broad range of ARGs were identified as the active resistance mobilome
564 across all hospital WW biofilm samples. These plasmids were mainly resistance plasmids found in Gram-
565 negative pathogens such as the $bla\text{-}_{VIM7}$ carrying plasmid *pmATVIM-7* first identified in *P. aeruginosa* (50);
566 the IncP-6 plasmid *Rms149,* a small resistant plasmid associated with *P. aeruginosa* (58) (detected only in
567 hospital *in situ* biofilm); several small resistance plasmids (e.g. *pKMA757, pARD3079, pKMA202,* and
568 *pKMA5)* associated with *Actinobacilli* (59) and plasmid families representing the groups IncP, F, N and Q
569 (Supplementary Figure 11). They primarily expressed aminoglycoside, sulphonamide, chloramphenicol,
570 and beta-lactam resistance genes (Supplementary Figure 11, Figure 6). 14 plasmids were detected in all
571 hospital WW biofilm samples, and 7 additional plasmids were only shared between the *in situ* hospital
572 WW biofilms and the *in vitro* hospital WW biofilm exposed to ciprofloxacin (Supplementary Figure 11).
573 Interestingly, 22 plasmids, carrying between 1 and 5 ARGs, were only identified in the *in vitro* hospital
574 WW biofilm exposed to ciprofloxacin (Supplementary Figure 11).

575 14 plasmids were unique for urban WW biofilm samples (*in situ* and *in vitro*). These plasmids mainly
576 carried macrolide and tetracycline resistance genes found in Gram-positive bacteria, such as Lactobacilli
577 (56). In addition, the *Enterococcus faecium* and *faecalis* plasmids *pRUM* and *pTEF1* were identified as
578 expressing both the macrolide resistance gene *ermB* (60–62) (Supplementary Figure 11). The broad host

579 range IncP-1 plasmid pKJK5 was also detected, expressing an aminoglycoside (*aadA6*) and a sulphonamide
580 (*sul1*) resistance gene (63,64). One Gram-negative multidrug resistance plasmid *pJR1* (65) was detected,
581 carrying the chloramphenicol resistance gene *catB2* and the tetracycline resistance gene *tet(G)*
582 (Supplementary Figure 11). Fifteen plasmids were uniquely identified in the *in situ* urban WW biofilm and
583 not in its *in vitro* counterpart. Five of these plasmids were also detected in the hospital WW biofilms
584 expressing different ARGs (e.g. *pJHCMW1* and *R46*), whereas they only carried a single ARG when detected
585 in the *in situ* urban biofilm (Supplementary Figure 11).

586 In the hospital WW biofilms, many plasmids were identified to carry multiple resistance genes (up to 5
587 ARGs carried on one MGE contig, Supplementary Figure 11). These genes mainly encoded resistance to
588 aminoglycosides, beta-lactams, sulphonamides, chloramphenicol, and quaternary ammonium
589 compounds (Figure 6, Supplementary Figure 11). For the urban WW biofilms, MGEs that express multiple
590 resistance genes were also identified, but with less ARGs associated (maximum three ARGs on one plasmid
591 in the *in situ* urban WW biofilm) (Supplementary Figure 11). The ARGs mainly detected in the active
592 resistance mobilome of urban WW biofilms were macrolide, tetracyclines and multi-drug efflux pumps
593 (Figure 6, Supplementary Figure 11). Contrary to what is observed for the effect of ciprofloxacin on the
594 active resistance mobilome of the *in vitro* hospital biofilm, less MGE-ARG associated contigs were
595 identified, and a much lower diversity of ARGs were expressed in the *in vitro* urban biofilm exposed to
596 ciprofloxacin (mainly macrolide resistance genes) (Supplementary Figure 11, Figure 6).

597 Overall, multivariate analyses of our mobilome data (correspondence analysis (CA) and in between CA
598 (bCA)), revealed a prominent association between the type of ARGs classes present on plasmids and their
599 biofilm origin. (*p*-value=0.026; Figure 6).

600

601

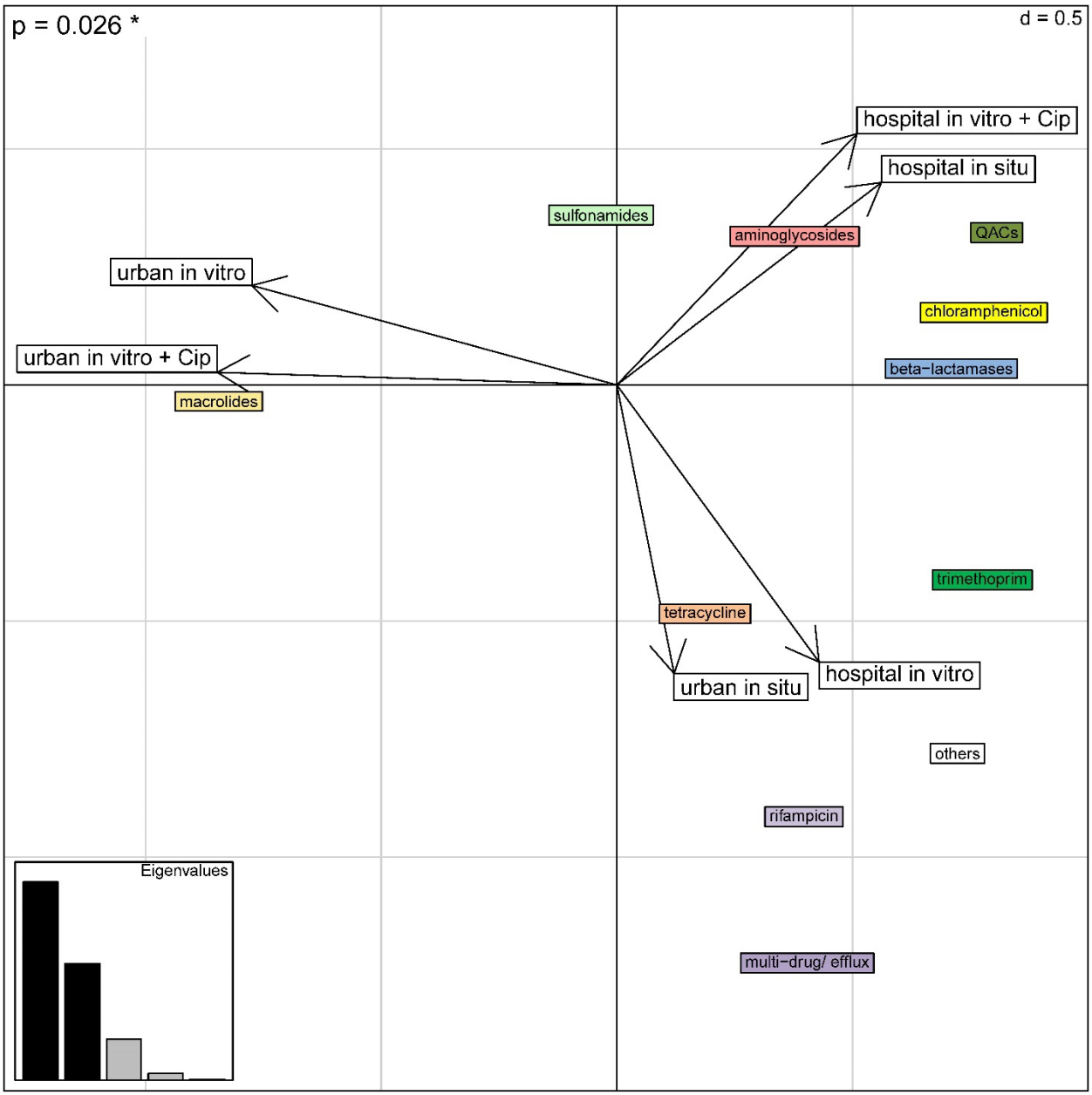

Figure 6: Between correspondence analysis (bCA) assessing the association between the type of ARGs classes present on plasmids, in terms of ARG class abundance (numbers of contigs) and the biofilm origin. This association represents 33% of the total association between biofilm origin and the ARGs composition of the mobilome identified by the CA (Supplementary Figure 12).

609 **Discussion**

610 The goal of this study was to develop a comprehensive experimental approach to assess WW biofilms as
611 putative hotspots for actual transfer of ARGs via MGEs within these communities using metagenomic
612 approaches. We furthermore wanted to quantify and visualize the EPS components of these biofilms, due
613 to the proposed role of the EPS in horizontal gene transfer within biofilms, as well as their relevance for
614 biofilms to tolerate antibiotics and exogeneous stressors (29,31,66–68).

615 Here we introduced a method by confocal laser scanning microscopy (CLSM) to visualize and quantify the
616 EPS of hospital and urban WW biofilms which will allow to study EPS components in these biofilms over
617 time and under different anthropogenic constraints. We showed that i) the EPS components investigated
618 are differentially abundant dependent on their growth environment (*in in* situ and *in vitro*) and their
619 sampling origin (hospital vs urban WW) and ii) ciprofloxacin at MSC impacted the quantity of the
620 measured EPS components. The decrease in the quantity of polysaccharides in the urban and in hospital
621 *in vitro* biofilms, and for eDNA in the hospital *in vitro* biofilm, due to the presence of ciprofloxacin might
622 be linked to a regulatory response of the biofilm community. In fact, it has been shown that exogeneous
623 stress in multi-species biofilms leads to decreased EPS production (69). External DNA was more abundant
624 in *in vitro* hospital WW biofilms compared to *in vitro* urban WW biofilms, which could be linked to higher
625 amounts of surfactants, antibiotics, and other pharmaceutical and chemical pollution in hospital WW (7)
626 that in turn may enhance bacterial lysis and active eDNA secretion in those biofilms (70). eDNA is known
627 to promote tolerance to antimicrobial agents in biofilms by inhibiting the diffusion of cationic molecules
628 (71) and by increasing the resistance to aminoglycosides in *Pseudomonas aeruginosa* biofilms (72,73). It
629 has also been shown that eDNA is involved in transfer of the ARG *tetM* by the conjugative transposon
630 Tn916 (68), through transformation. Transformation is suspected to be an important mechanism for gene
631 transfer between bacterial communities in biofilms (68). We showed that the microbiota of hospital and
632 urban WW biofilms is distinct, which is likely correlated to the different organization and relative
633 abundances detected for the EPS in the two WW biofilm niches, as shown by our analysis (Supplementary
634 Figure 5 and Supplementary Table 6). The significant increase of dead cells observed for the *in vitro*
635 hospital WW biofilm exposed to ciprofloxacin could be linked to the predominant Gram-negative genera
636 in hospital WW biofilms (Figure 3).

637 By implementing a meta-transcriptomic approach, at first, we wanted to assess the basic differential
638 expression levels of mobile genetic elements (MGEs) associated with ARGs as a proxy for actual transfer
639 of ARGs within hospital and urban WW biofilms. Second, we wanted to compare these levels to *in vitro*

640 reconstituted biofilms and third, we wanted to see whether these "basic" expression levels do change in
641 response to a single antibiotic added to the WW environment. Indeed, we showed that a) basic ARG and
642 MGEs expression levels are higher in *in situ* than *in vitro* WW hospital biofilms; b) expression levels of
643 ARGs and MGEs increase upon adding a minimal selective concentration (MSC) of ciprofloxacin to the *in*
644 *vitro* hospital WW biofilm environment and c) that expression of plasmids carrying specific ARG classes
645 and multiple ARGs at the same time, is associated with specific biofilm types (Figure 6). We were able to
646 detect a broad range of plasmids that were uniquely detected in either, hospital or urban WW biofilms,
647 hence correlated to their biofilm origin. Interestingly, plasmids that were detected in both, hospital and
648 urban *in situ* and *in vitro* biofilms, carried different types and quantities of ARGs (Supplementary Figure
649 9). This allowed us to identify a correlation between the nature of ARGs that are present on plasmids and
650 the biofilm environment and origin, and their likelihood to be actively expressed.

651 Interestingly, the reconstituted *in vitro* hospital and urban WW biofilms were more like each other
652 concerning their microbiota composition than their natural (*in situ*) biofilm counterparts. They differed
653 mainly in the relative abundance of their 3 main families (*Flavobacteriaceae*, *Comamonadaceae* and
654 *Pseudomonadaceae*) or genera (*Acinetobacter, Pseudomonas* and *Comamonas* for hospital *in vitro* WW
655 biofilms *and Acinetobacter, Pseudomonas* and *Flavobacterium* for urban *in vitro* biofilms, Figure 3). This
656 may suggest that the *in vitro* laboratory conditions promote similar biofilm formation for hospital and
657 urban WW biofilms, despite their originally quite different WW microbiota composition, which questions
658 our experimental set-up to implement microcosms in the laboratory that are capable to reproduce
659 ecosystem conditions identical to a natural environment. However, for example more frequent
660 refreshment of the WW alimentation in the *in vitro* system could significantly improve our experimental
661 model.

662 Among the classifiable rRNA reads from the meta-transcriptomic analysis (methods) we identified a large
663 majority of *Enterobacteriaceae* in the hospital biofilms, and a mix of *Flavobacteriaceae*,
664 *Enterobacteriaceae, Streptococaceae* and *Francisellaceae* in the urban *in situ* biofilm (Supplementary
665 Figure 6 and Supplementary Table 2). The fact that these rRNA reads were obtained from the RNA
666 sequencing run may indicate that these families were highly "active" in these biofilms although not highly
667 abundant based on 16S rDNA sequencing (Figure 3). The highly active proportion of *Enterobacteriaceae*
668 in hospital *in situ* and *in vitro* biofilms might indeed explain the higher expression levels and the types of
669 MGEs and ARGs detected in these samples, and their response to antibiotic stress. This further highlights
670 the need to study the 'active biofilm community' and might point towards the fact that the key players

671 for accumulation and transfer of ARGs and MGEs in highly anthropized sites such as WW are indeed
672 human-gut associated bacteria.

673 In a recent study, the Plascad tool was designed for plasmid classification, AMR gene annotation, and
674 plasmid visualization (74) and They showed that: i) most plasmid-borne ARGs, including those localized
675 on class-1 integrons, are enriched in conjugative plasmids in their datasets, and ii) transfer between AMR
676 plasmids and bacterial chromosomes was mediated by insertion sequences, mainly those belonging to
677 the IS6 family, IS26 and IS6100 (74). We have shown previously that IS26 and IS6100 were both abundant
678 in WW (7) and in this study we show that IS6100 is highly expressed in hospital WW biofilms. IS26 is
679 frequently detected in plasmids of clinical importance associated with antibiotic resistance genes.
680 Furthermore, IS26 has also been associated with the expression of antibiotic resistance genes (75). Finally,
681 the distinct plasmid profiles (Figure 6 and Supplementary Figure 11) and their specific ARG expression
682 profiles for hospital and urban WW biofilms point towards a strong environmental selection pressure
683 shaping the active resistance mobilome.

684 The strong correlation between high normalized abundance values of ARGs and the likelihood to be
685 detected by our meta-transcriptomic approach points towards limitations of RNA sequencing and
686 metatranscriptomics for the accurate quantification of ARGs and MGEs expression levels in complex multi-
687 species biofilm communities. The normalization of total ARG and MGEs reads allowed for the estimation
688 of those transcripts in the respective samples, and the comparison between the samples. However,
689 whether the "absence" of mRNA reads for ARGs, MGEs and specially ARGs detected to be on MGEs is due
690 to an insufficient sequencing depth cannot be excluded. Therefore, our analysis focused on the presence
691 of the ARG-MGE associated contigs, and their qualitative characteristics, which allowed for the detection
692 of significant correlations between the WW biofilm environment and sample origin, and to a slight degree,
693 the impact of antibiotic pressure on their presence and active transcription in the respective biofilms. Fast
694 progress is being made in the improvement of long-read third generation sequencing technologies, which
695 will allow for future validation of our findings, and the more accurate and in-depth study of hospital and
696 urban WW biofilms (76,77) and their differential expression of the "active resistance mobilome" in
697 response to exogeneous stress.

698 Here we provide an approach to comprehensively study multi-species biofilms that form in highly
699 anthropized environments such as WW. We show that hospital and urban wastewaters shape the
700 structure and active resistome of environmental biofilms, and we confirmed that hospital WW is an
701 important hot spot for the dissemination and selection of AMR. Hence, we propose that studying hospital

WW biofilms may present an ideal model to further unravel the complex correlation between pollution and AMR selection and the structural, ecological, functional, and genetic organization of multi-species biofilms as antibiotic resistance factories.

Data availability

16S rRNA sequence data are available at the European Nucleotide Archive (ENA) under the project number PRJEB59054. RNA sequencing data (metatranscriptomic data) will be available at the NCBI under submission number SUB12549421. All other important raw data needed to reconstruct the findings of our study are made available in the supplementary material.

Funding

E. Buelow has received funding from the European Union's Horizon 2020 research and innovation program under the Marie Skłodowska-Curie grant agreement RESOLVE 707999-standard EF.

Declaration of competing interest

The authors declare that they have no known competing financial interests or personal relationships that could have appeared to influence the work reported in this paper.

721 References

722 1. Balcazar JL, Subirats J, Borrego CM. The role of biofilms as environmental reservoirs of antibiotic
723 resistance. FrontMicrobiol. 2015;6(Journal Article):1216.

724 2. Hennequin C, Aumeran C, Robin F, Traore O, Forestier C. Antibiotic resistance and plasmid transfer
725 capacity in biofilm formed with a CTX-M-15-producing Klebsiella pneumoniae isolate.
726 JAntimicrobChemother. 2012;67(9):2123–30.

727 3. Ferreira C, Veldhoen M. Host and microbes date exclusively. Cell. 2012;149(7):1428–30.

728 4. Abe K, Nomura N, Suzuki S. Biofilms: hot spots of horizontal gene transfer (HGT) in aquatic
729 environments, with a focus on a new HGT mechanism. FEMS Microbiology Ecology [Internet]. 1.
730 Mai 2020 [zitiert 4. März 2021];96(fiaa031). Verfügbar unter:
731 https://doi.org/10.1093/femsec/fiaa031

732 5. Allen HK, Donato J, Wang HH, Cloud-Hansen KA, Davies J, Handelsman J. Call of the wild: antibiotic
733 resistance genes in natural environments. NatRevMicrobiol. 2010;8(4):251–9.

734 6. Flandroy L, Poutahidis T, Berg G, Clarke G, Dao MC, Decaestecker E, u. a. The impact of human
735 activities and lifestyles on the interlinked microbiota and health of humans and of ecosystems.
736 SciTotal Environ. 2018;627(Journal Article):1018–38.

737 7. Buelow E, Rico A, Gaschet M, Lourenço J, Kennedy SP, Wiest L, u. a. Hospital discharges in urban
738 sanitation systems: Long-term monitoring of wastewater resistome and microbiota in relationship
739 to their eco-exposome. Water Research X. 1. Mai 2020;7:100045.

740

741 8. Harris S, Morris C, Morris D, Cormican M, Cummins E. The effect of hospital effluent on
742 antimicrobial resistant E. coli within a municipal wastewater system. EnvironSciProcessImpacts.
743 2013;15(3):617–22.

744 9. Jia A, Wan Y, Xiao Y, Hu J. Occurrence and fate of quinolone and fluoroquinolone antibiotics in a
745 municipal sewage treatment plant. Water Research. 1. Februar 2012;46(2):387–94.

746 10. Hayes A, May Murray L, Catherine Stanton I, Zhang L, Snape J, Hugo Gaze W, u. a. Predicting
747 selection for antimicrobial resistance in UK wastewater and aquatic environments: Ciprofloxacin
748 poses a significant risk. Environment International. 1. November 2022;169:107488.

749 11. Kim D, Nguyen LN, Oh S. Ecological impact of the antibiotic ciprofloxacin on microbial community
750 of aerobic activated sludge. Environ Geochem Health. 1. Juni 2020;42(6):1531–41.

751 12. Nakata H, Kannan K, Jones PD, Giesy JP. Determination of fluoroquinolone antibiotics in
752 wastewater effluents by liquid chromatography–mass spectrometry and fluorescence detection.
753 Chemosphere. 1. Februar 2005;58(6):759–66.

754 13. Beaber JW, Hochhut B, Waldor MK. SOS response promotes horizontal dissemination of antibiotic
755 resistance genes. Nature. Januar 2004;427(6969):72–4.

14. Guerin É, Cambray G, Sanchez-Alberola N, Campoy S, Erill I, Re SD, u. a. The SOS Response Controls Integron Recombination. Science. 22. Mai 2009;324(5930):1034–1034.

15. Hu Y, Yang X, Qin J, Lu N, Cheng G, Wu N, u. a. Metagenome-wide analysis of antibiotic resistance genes in a large cohort of human gut microbiota. NatCommun. 2013;4(Journal Article):2151.

16. Forslund K, Sunagawa S, Coelho LP, Bork P. Metagenomic insights into the human gut resistome and the forces that shape it. Bioessays. 2014;36(3):316–29.

17. Sommer MO, Church GM, Dantas G. The human microbiome harbors a diverse reservoir of antibiotic resistance genes. Virulence. 2010;1(4):299–303.

18. Karkman A, Parnanen K, Larsson DGJ. Fecal pollution can explain antibiotic resistance gene abundances in anthropogenically impacted environments. NatCommun. 2019;10(1):80-018-07992–3.

19. Pehrsson EC, Forsberg KJ, Gibson MK, Ahmadi S, Dantas G. Novel resistance functions uncovered using functional metagenomic investigations of resistance reservoirs. FrontMicrobiol. 2013;4(Journal Article):145.

20. McInnes RS, uz-Zaman MH, Alam IT, Ho SFS, Moran RA, Clemens JD, u. a. Metagenome-Wide Analysis of Rural and Urban Surface Waters and Sediments in Bangladesh Identifies Human Waste as a Driver of Antibiotic Resistance. mSystems [Internet]. 13. Juli 2021 [zitiert 17. Dezember 2021]; Verfügbar unter: https://journals.asm.org/doi/abs/10.1128/mSystems.00137-21

21. Singer AC, Shaw H, Rhodes V, Hart A. Review of Antimicrobial Resistance in the Environment and Its Relevance to Environmental Regulators. FrontMicrobiol. 2016;7(Journal Article):1728.

22. Manaia CM, Rocha J, Scaccia N, Marano R, Radu E, Biancullo F, u. a. Antibiotic resistance in wastewater treatment plants: Tackling the black box. EnvironInt. 2018;115(Journal Article):312–24.

23. Rizzo L, Manaia C, Merlin C, Schwartz T, Dagot C, Ploy MC, u. a. Urban wastewater treatment plants as hotspots for antibiotic resistant bacteria and genes spread into the environment: a review. SciTotal Environ. 2013;447(Journal Article):345–60.

24. Haenni M, Dagot C, Chesneau O, Bibbal D, Labanowski J, Vialette M, u. a. Environmental contamination in a high-income country (France) by antibiotics, antibiotic-resistant bacteria, and antibiotic resistance genes: Status and possible causes. Environ Int. 15. Januar 2022;159:107047.

25. Luo YH, Lai YS, Zheng C, Ilhan ZE, Ontiveros-Valencia A, Long X, u. a. Increased expression of antibiotic-resistance genes in biofilm communities upon exposure to cetyltrimethylammonium bromide (CTAB) and other stress conditions. Science of The Total Environment. 15. April 2021;765:144264.

26. Proia L, von Schiller D, Sànchez-Melsió A, Sabater S, Borrego CM, Rodríguez-Mozaz S, u. a. Occurrence and persistence of antibiotic resistance genes in river biofilms after wastewater inputs in small rivers. Environmental Pollution. 1. März 2016;210:121–8.

792 27. Flemming HC, Wuertz S. Bacteria and archaea on Earth and their abundance in biofilms. Nat Rev
793 Microbiol. April 2019;17(4):247–60.

794 28. Ratajczak M, Kaminska D, Dlugaszewska J, Gajecka M. Antibiotic Resistance, Biofilm Formation,
795 and Presence of Genes Encoding Virulence Factors in Strains Isolated from the Pharmaceutical
796 Production Environment. Pathogens. Februar 2021;10(2):130.

797 29. Flemming HC, Wingender J. The biofilm matrix. NatRevMicrobiol. 2010;8(9):623–33.

798 30. Xiao J, Koo H. Structural organization and dynamics of exopolysaccharide matrix and microcolonies
799 formation by Streptococcus mutans in biofilms. JApplMicrobiol. 2010;108(6):2103–13.

800 31. Soares A, Roussel V, Pestel-Caron M, Barreau M, Caron F, Bouffartigues E, u. a. Understanding
801 Ciprofloxacin Failure in Pseudomonas aeruginosa Biofilm: Persister Cells Survive Matrix Disruption.
802 Front Microbiol. 13. November 2019;10:2603.

803 32. Buelow E, Bayjanov JR, Majoor E, Willems RJL, Bonten MJM, Schmitt H, u. a. Limited influence of
804 hospital wastewater on the microbiome and resistome of wastewater in a community sewerage
805 system. FEMS MicrobiolEcol. 2018;(Journal Article).

806 33. Chonova T, Lecomte V, Bertrand-Krajewski JL, Bouchez A, Labanowski J, Dagot C, u. a. The SIPIBEL
807 project: treatment of hospital and urban wastewater in a conventional urban wastewater
808 treatment plant. EnvironSciPollutResInt. 2018;25(10):9197–206.

809 34. Bengtsson-Palme J, Larsson DG. Concentrations of antibiotics predicted to select for resistant
810 bacteria: Proposed limits for environmental regulation. EnvironInt. 2016;86(Journal Article):140–9.

811 35. Buelow E, Bello Gonzalez TDJ, Fuentes S, de Steenhuijsen Piters WAA, Lahti L, Bayjanov JR, u. a.
812 Comparative gut microbiota and resistome profiling of intensive care patients receiving selective
813 digestive tract decontamination and healthy subjects. Microbiome. 2017;5(1):88-017-0309-z.

814 36. Bankevich A, Nurk S, Antipov D, Gurevich AA, Dvorkin M, Kulikov AS, u. a. SPAdes: a new genome
815 assembly algorithm and its applications to single-cell sequencing. J Comput Biol. Mai
816 2012;19(5):455–77.

817 37. Wood DE, Salzberg SL. Kraken: ultrafast metagenomic sequence classification using exact
818 alignments. Genome Biology. 3. März 2014;15(3):R46.

819 38. Pruesse E, Quast C, Knittel K, Fuchs BM, Ludwig W, Peplies J, u. a. SILVA: a comprehensive online
820 resource for quality checked and aligned ribosomal RNA sequence data compatible with ARB.
821 Nucleic Acids Res. 2007;35(21):7188–96.

822 39. Solden L, Lloyd K, Wrighton K. The bright side of microbial dark matter: lessons learned from the
823 uncultivated majority. Curr Opin Microbiol. Juni 2016;31:217–26.

824 40. Evaluation of metatranscriptomic protocols and application to the study of freshwater microbial
825 communities - Tsementzi - 2014 - Environmental Microbiology Reports - Wiley Online Library
826 [Internet]. [zitiert 22. Dezember 2022]. Verfügbar unter:
827 https://sfamjournals.onlinelibrary.wiley.com/doi/abs/10.1111/1758-2229.12180

828 41. Alcock BP, Raphenya AR, Lau TTY, Tsang KK, Bouchard M, Edalatmand A, u. a. CARD 2020:
829 antibiotic resistome surveillance with the comprehensive antibiotic resistance database. Nucleic
830 Acids Res. 8. Januar 2020;48(D1):D517–25.

831 42. Okshevsky M, Meyer RL. Evaluation of fluorescent stains for visualizing extracellular DNA in
832 biofilms. Journal of Microbiological Methods. 1. Oktober 2014;105:102–4.

833 43. Hothorn T, Bretz F, Westfall P. Simultaneous inference in general parametric models. Biom J. Juni
834 2008;50(3):346–63.

835 44. Using observation-level random effects to model overdispersion in count data in ecology and
836 evolution [PeerJ] [Internet]. [zitiert 22. Dezember 2022]. Verfügbar unter:
837 https://peerj.com/articles/616/

838 45. Jakobsson M, Edge MD, Rosenberg NA. The Relationship Between FST and the Frequency of the
839 Most Frequent Allele. Genetics. Februar 2013;193(2):515–28.

840 46. Toleman MA, Rolston K, Jones RN, Walsh TR. blaVIM-7, an Evolutionarily Distinct Metallo-β-
841 Lactamase Gene in a Pseudomonas aeruginosa Isolate from the United States. Antimicrob Agents
842 Chemother. Januar 2004;48(1):329–32.

843 47. Manchanda V, Sanchaita S, Singh N. Multidrug Resistant Acinetobacter. J Glob Infect Dis.
844 2010;2(3):291–304.

845 48. Vandewalle JL, Goetz GW, Huse SM, Morrison HG, Sogin ML, Hoffmann RG, u. a. Acinetobacter,
846 Aeromonas and Trichococcus populations dominate the microbial community within urban sewer
847 infrastructure. EnvironMicrobiol. 2012;14(9):2538–52.

848 49. Fisher JC, Levican A, Figueras MJ, McLellan SL. Population dynamics and ecology of Arcobacter in
849 sewage. FrontMicrobiol. 2014;5(Journal Article):525.

850 50. Ferreira S, Fraqueza MJ, Queiroz JA, Domingues FC, Oleastro M. Genetic diversity, antibiotic
851 resistance and biofilm-forming ability of Arcobacter butzleri isolated from poultry and
852 environment from a Portuguese slaughterhouse. IntJFood Microbiol. 2013;162(1):82–8.

853 51. Batovska J, Mee PT, Lynch SE, Sawbridge TI, Rodoni BC. Sensitivity and specificity of
854 metatranscriptomics as an arbovirus surveillance tool. Sci Rep. 18. Dezember 2019;9(1):19398.

855 52. Sivalingam P, Poté J, Prabakar K. Extracellular DNA (eDNA): Neglected and Potential Sources of
856 Antibiotic Resistant Genes (ARGs) in the Aquatic Environments. Pathogens. 23. Oktober
857 2020;9(11):874.

858 53. Eramo A, Medina WRM, Fahrenfeld NL. Viability-based quantification of antibiotic resistance genes
859 and human fecal markers in wastewater effluent and receiving waters. The Science of the total
860 environment. 3. März 2019;656:495.

861 54. Haines AS, Jones K, Cheung M, Thomas CM. The IncP-6 plasmid Rms149 consists of a small
862 mobilizable backbone with multiple large insertions. J Bacteriol. Juli 2005;187(14):4728–38.

863 55. Matter D, Rossano A, Sieber S, Perreten V. Small multidrug resistance plasmids in Actinobacillus
864 porcitonsillarum. Plasmid. 1. März 2008;59(2):144–52.

865 56. Mills S, McAuliffe OE, Coffey A, Fitzgerald GF, Ross RP. Plasmids of lactococci – genetic accessories
866 or genetic necessities? FEMS Microbiology Reviews. 1. März 2006;30(2):243–73.

867 57. Røder HL, Hansen LH, Sørensen SJ, Burmølle M. The impact of the conjugative IncP-1 plasmid
868 pKJK5 on multispecies biofilm formation is dependent on the plasmid host. FEMS Microbiol Lett.
869 Juli 2013;344(2):186–92.

870 58. Popowska M, Krawczyk-Balska A. Broad-host-range IncP-1 plasmids and their resistance potential.
871 Frontiers in Microbiology [Internet]. 2013 [zitiert 11. Juli 2022];4. Verfügbar unter:
872 https://www.frontiersin.org/articles/10.3389/fmicb.2013.00044

873 59. Wu JR, Shieh HK, Shien JH, Gong SR, Chang PC. Molecular characterization of plasmids with
874 antimicrobial resistant genes in avian isolates of Pasteurella multocida. Avian Dis. Dezember
875 2003;47(4):1384–92.

876 60. Karygianni L, Ren Z, Koo H, Thurnheer T. Biofilm Matrixome: Extracellular Components in
877 Structured Microbial Communities. Trends in Microbiology. 1. August 2020;28(8):668–81.

878 61. Gu C, Gao P, Yang F, An D, Munir M, Jia H, u. a. Characterization of extracellular polymeric
879 substances in biofilms under long-term exposure to ciprofloxacin antibiotic using fluorescence
880 excitation-emission matrix and parallel factor analysis. Environ Sci Pollut Res. 1. Mai
881 2017;24(15):13536–45.

882 62. Hannan S, Ready D, Jasni AS, Rogers M, Pratten J, Roberts AP. Transfer of antibiotic resistance by
883 transformation with eDNA within oral biofilms. FEMS Immunology & Medical Microbiology. 1.
884 August 2010;59(3):345–9.

885 63. Loustau E, Leflaive J, Boscus C, Amalric Q, Ferriol J, Oleinikova O, u. a. The Response of
886 Extracellular Polymeric Substances Production by Phototrophic Biofilms to a Sequential
887 Disturbance Strongly Depends on Environmental Conditions. Frontiers in Microbiology [Internet].
888 2021 [zitiert 21. November 2022];12. Verfügbar unter:
889 https://www.frontiersin.org/articles/10.3389/fmicb.2021.742027

890 64. Okshevsky M, Meyer RL. The role of extracellular DNA in the establishment, maintenance and
891 perpetuation of bacterial biofilms. Critical Reviews in Microbiology. 3. Juli 2015;41(3):341–52.

892 65. Wilton M, Charron-Mazenod L, Moore R, Lewenza S. Extracellular DNA Acidifies Biofilms and
893 Induces Aminoglycoside Resistance in Pseudomonas aeruginosa. Antimicrobial Agents and
894 Chemotherapy. 31. Dezember 2015;60(1):544–53.

895 66. Doroshenko N, Tseng BS, Howlin RP, Deacon J, Wharton JA, Thurner PJ, u. a. Extracellular DNA
896 impedes the transport of vancomycin in Staphylococcus epidermidis biofilms preexposed to
897 subinhibitory concentrations of vancomycin. AntimicrobAgents Chemother. 2014;58(12):7273–82.

898 67. Lewenza S. Extracellular DNA-induced antimicrobial peptide resistance mechanisms in
899 Pseudomonas aeruginosa. Front Microbiol. 14. Februar 2013;4:21.

900 68. Che Y, Yang Y, Xu X, Břinda K, Polz MF, Hanage WP, u. a. Conjugative plasmids interact with
901 insertion sequences to shape the horizontal transfer of antimicrobial resistance genes. Proc Natl
902 Acad Sci USA. 9. Februar 2021;118(6):e2008731118.

903 69. Yang M, Cousineau A, Liu X, Luo Y, Sun D, Li S, u. a. Direct Metatranscriptome RNA-seq and
904 Multiplex RT-PCR Amplicon Sequencing on Nanopore MinION – Promising Strategies for Multiplex
905 Identification of Viable Pathogens in Food. Front Microbiol. 9. April 2020;11:514.

906 70. Liu L, Yang Y, Deng Y, Zhang T. Nanopore long-read-only metagenomics enables complete and
907 high-quality genome reconstruction from mock and complex metagenomes. Microbiome. 2.
908 December 2022;10(1):209.

909

910

911